

Fibre strength selection and the mechanical resistance of fibre-reinforced metal matrix composites

L. PAMBAGUIAN, R. MEVREL

ONERA, Direction des matériaux, 29 avenue de la Division Leclerc, B.P. 72, 92322 Châtillon Cedex, France

For predicting the strength of fibre-reinforced metal matrix composites, the *in situ* fibre strength value has to be introduced in the calculations. Tension tests series have been conducted on SiC fibres (SCSO and SCS2 TEXTRON) before and after chemical interaction with a pure liquid aluminium bath and the reacted fibres have been tested before and after dissolution of the aluminium coating simulating the metallic matrix around the fibres. The results obtained for the different fibre batches show that the *in situ* fibre resistance may differ significantly from the strength of as-received or extracted fibres that is usually adopted in the models.

1. Introduction

The interest in fibre-reinforced metal matrix composites (FRMMCs) stems from their potential as a high-strength material and, given an appropriate combination of reinforcement and light metal matrix, as a material of high specific strength. The FRMMCs' strengths depend to a large extent on fibre strength and also on interfacial properties and matrix load bearing efficiency, i.e. the way fibres are loaded around a fibre breakage, [1-3].

The rule of mixtures is often used [4-9] to evaluate the upper limit of composite strength, σ_c

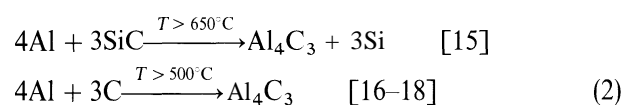
$$\sigma_c = V_f \sigma_f + (1 - V_f) \sigma_m \quad (1)$$

where: σ_f is the strength of the filament, σ_m the strength of the matrix, and V_f the volume fraction of the fibres.

Usually, the value adopted for the matrix strength is derived from the metallic alloy bulk strength, although some studies have shown that the presence of a reinforcement could modify the matrix microstructure and therefore its properties. For example, the presence of a reinforcement can limit grain growth [10-12]. Flon and Arsenault [13] report a large plastic deformation zone of a pure aluminium matrix around a single silicon carbide fibre during composite cooling down. Salvo [14] explains that, around fibres, matrix yielding changes the hardening precipitation structure and therefore the yield strength of the matrix. Nevertheless, the matrix contribution to composite strength remains relatively low and those effects are therefore negligible.

The fabrication process can affect the fibre resistance much more strongly. In the case of carbon and silicon carbide fibres, for example, the following reactions occur at high temperature, with aluminium

based matrix alloys



According to [15] they proceed via a dissolution-crystallization process: in the first reaction, for example, carbon dissolves and migrates in liquid aluminium. The aluminium carbides grow on the matrix side. This reaction mechanism can explain why the aluminium carbide never forms a continuous layer, which could act eventually as a diffusion barrier and thereby could slow down the reaction. So, in this case, the longer the time or the higher the temperature, the more affected the fibre is by reaction products.

As far as the fibre strength value is concerned, in principle, the strength of the fibre *in situ* should be adopted for predicting the properties of the composite, in particular its strength. To the authors' knowledge, the influence of the reaction layer is not taken into account and either the strength of the as-received fibres [4-8] or the strength of extracted fibres is selected [9].

In this paper the authors attempt to evaluate this effect and focus attention on the fibre strength value to be adopted for predicting the composite ultimate strength. A model system has been selected, constituted of silicon carbide fibres (TEXTRON SCSO and SCS2) and a pure (99.99%) aluminium matrix. The fibres have been mechanically tested under different conditions

1. as-received,
2. coated with a thin film of aluminium matrix, and
3. after dissolution of this aluminium film.



Figure 1 Scheme of the fibre sample test.

The results obtained are then discussed to explain how the composite manufacturing process may affect fibre strength in aluminium matrix composites.

2. Experimental procedure

2.1. Fibres

Two TEXTRON fibres (SCSO and SCS2) elaborated by chemical vapour deposition, have been considered in this study. Their structure is complex and it comprises

1. a carbon core (33 μm diameter) coated, to smooth its surface, with a 1 μm thick layer of pyrolytic carbon;
2. a shell of silicon carbide deposited by chemical vapour deposition (thickness: 52.5 μm); and
3. in the case of SCS2, a 1 μm thick external deposit (simply referred to later as the SCS2 layer) especially designed for incorporation in aluminium alloy matrix (it is mainly constituted of pyrolytic carbon and silicon carbide grains [19]).

2.2. Experimental description

2.2.1. *Manufacture*

Fibres have been coated with a thin (about 2 μm thick) layer of aluminium by dipping them for 4 min in a liquid aluminium bath held at 700 $^{\circ}\text{C}$. The time and temperature ranges are typical of those met in infiltration processes developed for fabricating fibre reinforced metal matrix composites [20,21]. A number of these coated fibres have been immersed in a 10% hydrochloric acid solution for 48 h to remove the aluminium layer as well as the aluminium carbide crystals if present.

Three fibre populations have thus been tested

1. as-received (noted AR),
2. coated with a thin aluminium layer (noted + Al), and
3. coated with an aluminium layer subsequently removed (noted - Al).

2.2.2. *Tensile testing*

The mechanical tests have been conducted on a classical screw type machine equipped with a 100 N load cell. Fibre samples have been glued on two aligned pieces of aluminium, at the bottom of herringbone chevrons (Fig. 1). The deformation speed was constant, and was equal to 10^{-4}s^{-1} . The test was considered valid if fibre rupture occurred outside the glued zone and if the force-deformation curve exhibited regular variations.

For each type of fibre, two gauge lengths were tested, 25 and 50 mm. Longer fibres could not be treated uniformly in the furnace and manipulation of shorter fibres was very difficult in the case of less resistant fibres.

r or each series 50 tests were performed out of which about more than 40 were valid.

2.2.3. *Data exploitation*

Ceramic fibre strength depends on flaw population. A single fibre failure happens when the most severe flaw present can propagate. The presence probability of a critical flaw is proportional to the specimen length and in order to determine fibre strength distribution, a Weibull [22] statistical approach has been used (Equation 3)

$$Pr(\sigma) = 1 - \exp\left[-\left(\frac{\sigma}{\sigma_0}\right)^m\right] \quad (3)$$

where $Pr(\sigma)$ is the rupture probability for a stress lower than σ ; m is the Weibull modulus (the lower m , is the wider the strength distribution); and σ_0 is the scaling parameter, taking into account the sample length.

Different methods can be used to derive the Weibull parameters m and σ_0 from experimental results. From the simulation study in [23], it appears that a satisfactory convergence can be obtained for the Weibull modulus with about 40 rupture strength results. It must be noted, however, that the modulus calculated from a single series is contained in a $\pm 20\%$ interval around the true value of m for a confidence level of 95%.

Equation 3 has been rearranged to give a linear dependence between $Pr(\sigma)$ and σ , with a slope equal to m

$$\ln\{-\ln[1 - Pr(\sigma)]\} = m[\ln(\sigma) - \ln(\sigma_0)] \quad (4)$$

The rupture probability has been determined using as an estimator

$$Pr(\sigma) = \frac{i}{(N + 1)} \quad (5)$$

where i is the number of tests where fibre strength is lower than σ , and N is the total number of tests.

In order to eliminate the non-significant traction test results, the Weibull fibre strength distribution has been assimilated to a Gaussian distribution. The values outside the range $[(\sigma) - 3s; (\sigma) + 3s]$ with $\langle\sigma\rangle$ the average strength and s the standard deviation, have been rejected.

3. Results and discussion

The results obtained are illustrated, for 25 mm gauge length, on Figs 2 and 3. The trends are similar for 50 mm gauge length. Fig. 2 presents the Weibull plot of rupture stress data for the six types of fibre, the corresponding strength histograms are reported on Fig. 3. Data for both fibre lengths are summarized in Tables I-III.

3.1. As-received fibres (AR)

3.1.1. *AR SCSO fibre*

The Weibull plot corresponding to SCSO AR is characteristic of a single flaw population. This is confirmed

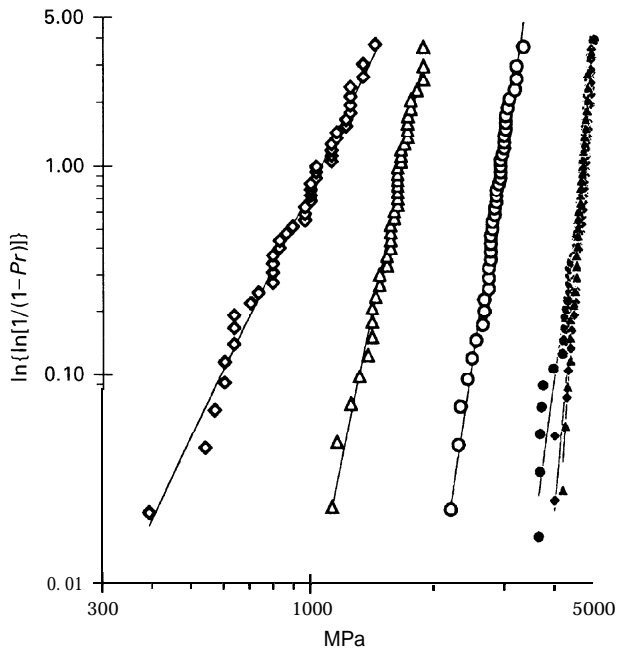


Figure 2 Weibull plots of the six batches of fibres, gauge length 25 mm. (○) SCSO AR, (◇) SCSO + Al, (△) SCSO - Al, (●) SCS2 AR, (◆) SCS2 + Al, (▲) SCS2 - Al.

TABLE I Average strength and Weibull modulus of the different as received fibres tested

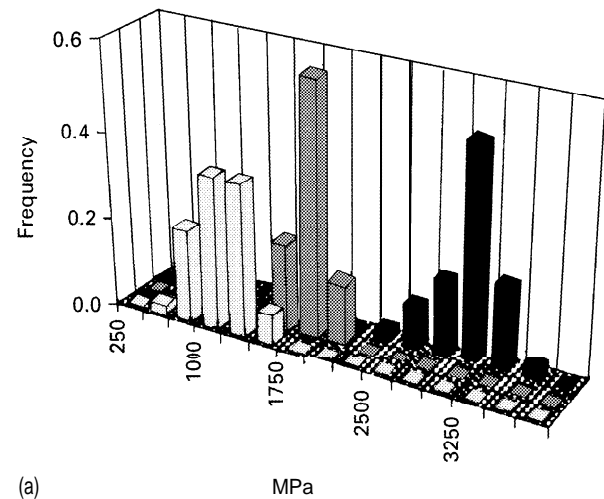
AR fibres (mm)	$\langle\sigma_r\rangle$ (MPa)	m
s c s o 50	2620	11.7
s c s o 25	2950	12.5
s c s 2 50	4450	10.9
SCS2 25	4700	13.9

TABLE II Average strength and Weibull modulus of the different + Al fibres tested

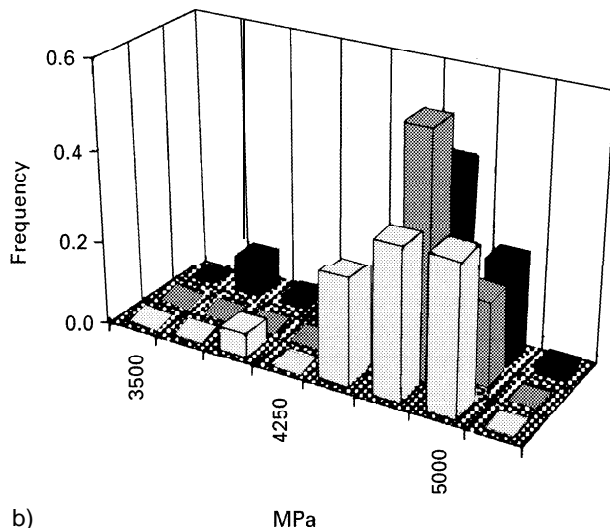
+ Al fibres (mm)	$\langle\sigma_r\rangle$ (MPa)	m
s c s o 50	940	4.0
SCSO 25	950	4.0
s c s 2 50	4540	26.0
SCS2 25	4670	28.2

TABLE III Average strength and Weibull modulus of the different - Al fibres tested

- Al fibres (mm)	$\langle\sigma_r\rangle$ (MPa)	m
s c s o 50	1580	19.8
s c s o 25	1580	9.4
s c s 2 50	4450	25.5
SCS2 25	4600	27.4



(a)



(b)

Figure 3 Rupture strength histograms of the six batches of fibres: (a) SCSO fibres, and (b) SCS2 fibres; gauge length 25 mm. (■) + Al, (□) - Al, (●) AR.

by the aspect of the rupture strength histogram which presents only one maximum.

3.1.2. AR SCS2 fibre

On the SCS2 AR fibre Weibull plot, the experimental points corresponding to the lower strength values deviate from the linear regression. The presence of two maxima (at about 4 and 4.7 GPa) on the rupture strength histogram indicates that fibre rupture could be due to two flaw populations. In such a case, it is impossible to determine the Weibull parameter of each flaw population except if the corresponding rupture strength distributions are well separated [24]. However, tests series carried out with longer (100 mm) and shorter (16 mm) gauge lengths have not permitted the separation of the two strength distributions.

3.1.3. Difference between AR SCSO and AR SCS2

One can see on Table I that the SCS2 fibre is much more resistant (about 160%) than the SCSO fibre. This improvement can only be explained by the presence of the SCS2 layer. In the case of the SCSO fibre, the rupture originates from flaws located on the silicon carbide surface. The SCS2 layer, by modifying this surface, tends to heal partially these defects.

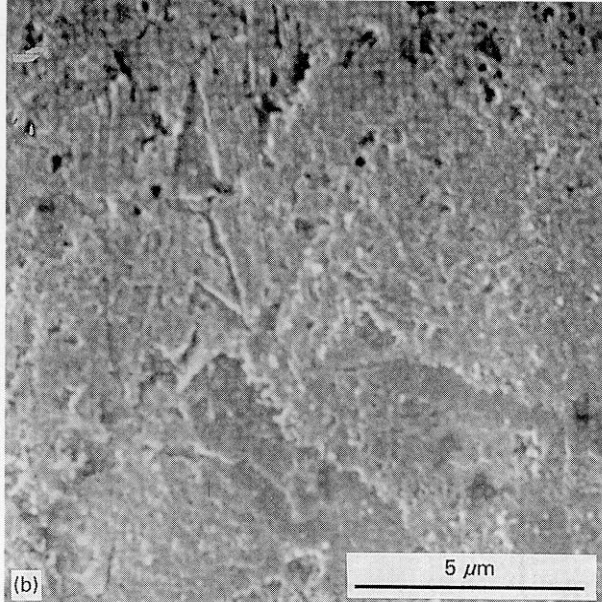
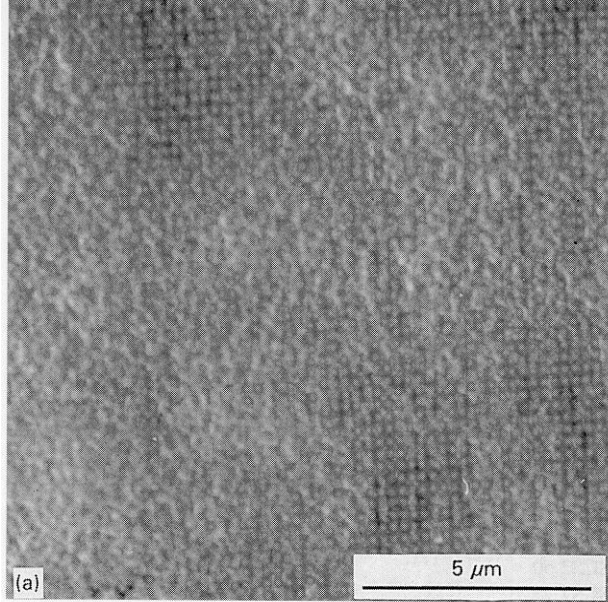


Figure 4 Aspect of the SCSO fibre surface: (a) AR and (b) - Al.

3.2. Fibres covered by a thin aluminium film (+ Al fibres)

3.2. 1.+Al SCSO fibre

Comparison of Tables I and II shows that the SCSO fibre is significantly altered as a result of its interaction with liquid aluminium. **After treatment**, its average strength is about 2.5 times lower than as-received. During fibre-metal interaction, only the silicon carbide surface can be modified by reaction product formation. So, the rupture of + Al SCSO fibre is controlled by flaws located near the fibre-metal interface. The Weibull modulus of this flaw population is significantly less than the one corresponding to the initial surface defects.

3.2.2. +Al SCS2 fibre

The average strengths of as-received and aluminium coated SCS2 fibres are nearly the same (Tables I and II), meaning that fibre-matrix chemical interaction has an insignificant effect on fibre strength. On the other hand, the Weibull modulus of the + Al fibre population is much higher (above 25) than the AR fibre population (about 10-15), indicating that chemical reaction between the fibre and the matrix modifies the fibre surface. This observation is confirmed by the rupture strength histograms. One can see that the lower strength values obtained with the AR fibre are no longer present on the histogram corresponding to the + Al fibre. One can deduce therefore that the more severe flaws in AR SCS2 fibres are located on the fibre surface and their effect is much less pronounced after fibre-matrix interaction.

3.2.3. Comparison between +Al SCS2 and +Al SCSO

The behaviour of both fibres during fibrematrix reaction is very different. With the SCSO fibre, immer-

sion leads to the formation of a new flaw population near the fibre-metal interface. As a consequence, fibre resistance and Weibull modulus are less than before. On the contrary, the rupture strength of the SCS2 fibre remains unaffected by fibre-metal interaction. The chemical reaction seems to erase partially the defects on the fibre surface, leading to an increase of the Weibull modulus.

3.3. Fibres after aluminium film dissolution (-Al fibres)

3.3. 1.-Al SCSO fibre

The - Al SCSO fibre strength is approximately half the AR one. It is also 1.6 times higher than the + Al one.

The difference in behaviour between AR and - Al SCSO fibres can be explained easily. As can be seen on Fig. 4a and b, the surface of the - Al fibre presents much bigger defects than the AR one. The presence of these surface defects can explain the difference in strength between these fibres as well as the evolution of the Weibull modulus.

It is more difficult to explain the difference between + Al and -Al fibres. The difference in strength between + Al and - Al fibres can only be attributed to aluminium-fibre reaction products. As can be seen on Tables I and II, the presence of those products strongly decreases the Weibull modulus, revealing a wider distribution in the flaws located on the silicon carbide surface when interfacial products are present.

According to [15], only the aluminium carbide can be formed at the silicon carbide-aluminium interface. This compound has been observed by optical microscopy (Fig. 5) as a 1 μm thick layer. During a traction test, this layer generated local overstresses in the fibre. Different mechanisms may cause the following.

1. Aluminium carbide crystals to rupture: if it happens before silicon carbide rupture, a crack is

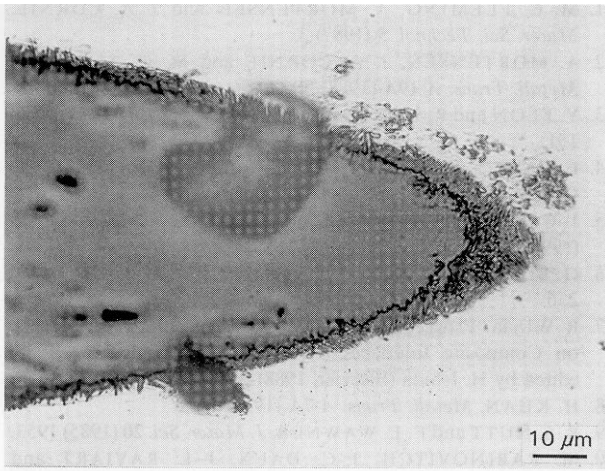


Figure 5 Aluminium carbides located at the SCSO–aluminium interface.

nucleated. The length of this crack is of the order of the aluminium carbide length.

2. Thermally induced stresses: if the thermal expansion coefficient of silicon carbide is higher than the aluminium carbide one, a tensile stress appears in the fibre near the aluminium carbide tip after cooling down from the manufacture temperature.

3. Stresses due to a positive volume mismatch: if the reaction product Al_4C_3 occupies a larger volume than silicon carbide from which it is formed.

1. With the aim of knowing the length that aluminium carbide particles should have to provoke fibre rupture under 950 MPa in mode I, the fibre has been assimilated to a finite plate with an open crack. For this geometry, the mode I critical overstress coefficient [25] is given by

$$K_{1C} = \sigma_r(\pi a)^{1/2} \left[\frac{2b}{\pi a} \tan\left(\frac{\pi a}{2b}\right) \right]^{1/2} \times \left[\frac{0.752 + 0.37[1 - \sin(\pi a/2b)]^3 + 2.02(a/b)}{\cos[\pi a/2b]} \right] \quad (6)$$

in which b is the fibre diameter and a represents the defect length. In the AR and $- \text{Al}$ fibre, a is equal to the surface flaw depth; in the $+ \text{Al}$ fibres, it is equal to the aluminium carbide length. As the a/b ratio is much smaller than unity, Equation 6 can be written as

$$K_{1C} \approx \sigma_r \pi^{1/2} [1.122a^{1/2} + 1974a^{3/2}] \quad (7)$$

For a toughness of $3.3 \text{ MPa m}^{1/2}$ (low value for silicon carbide toughness), the corresponding crack length is about 3 μm , i.e. three times the aluminium carbide layer thickness. If this can contribute to the observed effect, it therefore cannot explain it fully.

As an indication, the same calculus for AR fibre gives a crack length of about $0.05 \mu\text{m}$; which is realistic, but unfortunately difficult to detect by scanning electron microscopy.

2. The thermal expansion coefficient of aluminium carbide ($\alpha_{\text{Al}_4\text{C}_3} = 7 \times 10^{-6} \text{ K}^{-1}$ [26]) is higher than the value for silicon carbide ($\alpha_{\text{SiC}} < 5 \times 10^{-6} \text{ K}^{-1}$ [27]); therefore during the cool down the thermally

induced stress inside the silicon carbide shell would be compressive and would not participate in the degradation of the fibre strength.

3. As one can see on Fig. 5, aluminium carbides form as wedges in the silicon carbide fibre, indicating partial growth by transformation of the silicon carbide volume into the aluminium carbide volume. A simple calculation from the crystallographic data, as reported in ASTM cards No. 29-1129 and 35-799, shows that this transformation is accompanied by a volume increase of about 30%. This effect could result in stress concentration at this location. Furthermore, it is to be noted that both carbides seem to be bonded well together [28].

As a conclusion, it can be proposed that the deleterious effect of the reaction products on the fibre strength originates most probably from the combined effect of the volume mismatch (between aluminium and silicon carbide particles) and the increase in size of the surface defects.

3.3.2. $- \text{Al}$ SCS2 fibre

The comparison of $+ \text{Al}$ and $- \text{Al}$ SCS2 fibres (Tables II and III) indicates that the chemical reaction products at the fibre-matrix interface have practically no influence on fibre strength. The AR and $- \text{Al}$ fibre surface aspects are difficult to differentiate with scanning electron microscopy. This means that SCS2 layer reactivity with aluminium is low, preventing therefore fibre degradation by interfacial reaction product.

4. Conclusions

Sic-based fibres (SCSO and SCS2) have been dipped in an aluminium bath in conditions typical of the manufacture of metal matrix composites. The influence of fibre-matrix chemical interaction on fibre resistance has been studied by comparing fibres as-received, coated by a thin aluminium film and after dissolution of this aluminium film.

1. As regards the SCSO fibre, fibre-aluminium reactivity is high. Two mechanisms leading to strength loss have been pointed out. The formation of defects on the fibre surface during chemical interaction decreases its resistance by about 50%. The presence of these reaction products at the fibre-matrix interface generates local overstresses and decreases fibre resistance by a further 35%.

2. As for the SCS2 fibre, fibre-aluminium reactivity is low. The fibre is not damaged during its interaction with aluminium. Moreover, the formation of small size reaction products seems to heal the fibre surface. The most severe flaws located on the as-received fibre surface are removed after fibre-aluminium reaction.

From these results, the following conclusions can be drawn. If the fibres are not chemically sensitive to the elaboration process (case of the SCS2 fibres), the value of the fibre strength to be adopted in the composite strength estimation can be the one determined on extracted fibres. On the contrary, when the

fibre-matrix reactivity is high (the case of SCSO fibre in this study and most likely of high resistance carbon fibres) a new flaw population can appear on the fibre surface. These flaws, stigmata of interfacial compounds; can affect deeply the fibre resistance. The presence of reaction products can further alter the in situ fibre strength. These results show that, in such systems, it is essential that the evaluation of the fibre strength should be carried out in conditions representing the fibre environment inside the composite and values obtained from extracted fibres can be significantly misleading.

References

1. S. OCHIAI, K. OSAMURA and K. ABE, *Z. Metallde* **76** (1975) 402.
2. S. OCHIAI and K. OSAMURA, *ibid.* 79 (1988) 610.
S. OCHIAI, K. SCHULTE and P. W. M. PETERS, *Comp. Sci. Technol.* **41** (1991) 237.
4. A. P. LEVITT, E. DI CESARE and S. M. WOLF, *Metall. Trans.* **3** (1972) 2455.
Y. KAGAWA and E. NAKATA, *J. Mater. Sci. Lett.* **11** (1992) 176.
6. A. OKURA, J. INAGAKI, E. NAKATA, S. IKEGAMI, T. OHSAKI and M. YOSHIDA, in "Proceedings of the International Conference on Composite Materials 3 (ICCM3)", Paris, August 1980, edited by T. Hayashi (TMS-AIME, 1980) vol. 2, 281.
CHEN XIU-QI and GENG-XIANG, *Mater. Sci. Engng* **84** (1986) 171.
8. M. U. ISLAM and W. WALLACE, Report NCR No. 23498 (National Research Council, Ottawa, Canada, 1984).
9. G. D. ZHANG, S. R. FENG, Q. LI, J. T. BLUCHER and J. A. CORNIE, in "Proceedings of the Third International Conference on Composite Interfaces (ICCI-III)", Cleveland, May 1990, edited by H. Ishida (Elsevier, 1990) p. 343.
10. A. MORTENSEN, M. N. GUNGOR, J. A. CORNIE and M. C. FLEMING, *J. Metals* March (1986) 30.
11. M. C. FLEMING, A. MORTENSEN and J. A. CORNIE, *Mater. Sci. Technol.* **5** (1987) 3.
12. A. MORTENSEN, J. A. CORNIE and M. C. FLEMING, *Metall. Trans. A* **19A** (1988) 709.
13. Y. FLON and R. J. ARSENAULT, *Mater. Sci. Engng* **75** (1985) 151.
14. L. SALVO, PhD thesis, Institut National Polytechnique de Grenoble (1992).
15. J. C. VIALA, P. FORTIER and J. BOUIX, *J. Mater. Sci.* **25** (1990) 1842.
16. G. BLANKENBURGS, *J. Australasian Inst. Metals* **14** (1969) 236.
17. R. W. U., in "Proceedings of the Second International Conference on Composite Interfaces (ICCI-II)", Cleveland, June 1988, edited by H. Ishida (Elsevier, 1988) p. 43.
18. H. KHAN, *Metall. Trans. A* **7A** (1976) 1281.
19. R. S. NUTT and F. E. WAWNER, *J. Mater. Sci.* **20**(1985) 1953.
20. M. RABINOVITCH, J.-C. DAUX, J.-L. RAVIART and R. MEVREL, in "Proceedings of ECCM 4", Stuttgart, September 1990, edited by J. Fuller, G. Gruninger, K. Schulte, A. R. Bunsell and A. Massiah, (Elsevier, 1990) p. 405.
21. M. RABINOVITCH, J.-C. DAUX, J.-L. RAVIART, R. MEVREL, M.-H. VIDAL-SETIF, H. ABIVEN and J. F. PELTIER, in "Proceedings, International Symposium on Advanced Materials for Lightweight Structures ESTEC", Noordwijk, March 1992, (European Space Agency, Paris, 1992) p. 135.
22. W. WEIBULL, *J. Appl. Mech.* **18** (1951) 293.
23. S. VAN DER SWAAGT, *J. Test. and Eval.* **17** (1989) 292.
24. C. P. BEETZ, *Fibre Sci. Technol.* **16** (1992) 45.
25. B. BARTH ELEM Y, "Notions Pratiques de Mecanique de la Rupture" (Eyrolles, Paris, 1980) 83.
26. T. ISEKI, T. KAMEDA and T. MARUYAMA, *J. Mater. Sci. Lett.* **2** (1983) 675.
27. Z. LI and R. C. BRAD, *J. Am. Ceram. Soc.* **70** (1987) 445.
28. S. D. PETEVES, P. TAMBUIYSER, P. HELBACH, M. AUDIER, V. LAURENT and D. CHATAIN, *J. Mater. Sci.* **25** (1990) 3765.

Received 15 February 1995
and accepted 18 March 1996